phys. stat. sol. (b) **245**, No. 12, 2642–2648 (2008) / **DOI** 10.1002/pssb.200844227

physica status solidi b
www.pss-b.com
basic solid state physics

Multiscale simulation of polycrystal mechanics of textured β-Ti alloys using ab initio and crystal-based finite element methods

D. Ma*, M. Friák, J. Neugebauer, D. Raabe, and F. Roters

Max-Planck-Institut für Eisenforschung GmbH, Max-Planck-Str. 1, 40237 Düsseldorf, Germany

Received 30 May 2008, revised 1 October 2008, accepted 16 October 2008
Published online 7 November 2008

PACS 02.70.Dh, 62.20.Fe, 71.15.Mb

* Corresponding author: e-mail d.ma@mpie.de

Crystal-based finite element methods (FEM) are versatile continuum approaches for predicting mechanical properties and deformation-induced crystallographic textures. They can be applied to both, elastic–plastic and elastic problems. The methodology is based on (i) a detailed understanding of the underlying crystal deformation mechanisms and (ii) a number of constitutive material parameters that are often difficult to measure. First principle calculations, that take into account the discrete nature of matter at the atomic scale, are an alternative way to study mechanical properties of single crystals without using empirical parameters. In this study we demonstrate how to combine these two well-established modeling tools, viz., ab initio modeling and crystal mechanical FEM, for an improved approach to design of polycrystalline materials. The combination is based on (i) the determination of basic thermodynamic and elastic parameter trends in metallurgical alloy design using density-functional (DFT) calculations (P. Hohenberg and W. Kohn, Phys. Rev. **136**, B864 (1964), W. Kohn and L. J. Sham, Phys. Rev. **140**, A1133 (1965) [1, 2], respectively) and (ii) the up-scale transfer of these results into crystal-based finite element simulations which take into account the anisotropic nature of the elastic–plastic deformation of metals. The method is applied to three body-centered cubic (bcc, β) Ti–Nb alloys for bio-medical applications. The study addresses two technological processes, namely, the prediction of texture evolution during cold rolling (elastic-plastic problem) and elastic bending of textured polycrystals (elastic problem).

© 2008 WILEY-VCH Verlag GmbH & Co. KGaA, Weinheim

1 Introduction The application of bcc Ti-alloys for bone replacement applications has attracted great attention because of the low elastic modulus and biocompatibility of these alloys [3]. The first theoretical approach to β-Ti alloys design was proposed by Morinaga et al. [4, 5]. Although their work has proven very powerful for the design of novel β-Ti alloys, it did not provide quantitative information, such as for instance the minimum alloy composition that is required to stabilize the β-phase or the elastic constants of the resulting alloys. In this paper a bottom-up theoretical concept for the design of advanced β-Ti alloys is presented.

The starting point is the use of quantum-mechanical predictions based on density functional theory (DFT). The results of the DFT calculations, namely the elastic constants and the chemical composition, are subsequently used as input in crystal-based finite element simulations. The latter method comprises a group of continuum-based approaches which consider the tensorial nature of elastic-plastic crystalline deformation and the orientation distribution in a (poly-)crystalline aggregate. In the case of purely elastic problems the method is referred to as crystal elasticity finite element method (CEFEM) and in the case of elastic–plastic loading it is referred to as crystal plasticity finite element method (CPFEM) (Fig. 1). We apply both methods for the investigation of two engineering problems, Fig. 1.

The first one is the evolution of the crystallographic texture during elastic–plastic plane strain deformation (idealization for cold rolling) as a function of the magnitude and anisotropy of the elastic stiffness. The second one is the prediction of the overall elastic stiffness of a textured polycrystal in case of reversible bending for different elastic tensors.

WILEY InterScience® DISCOVER SOMETHING GREAT

© 2008 WILEY-VCH Verlag GmbH & Co. KGaA, Weinheim

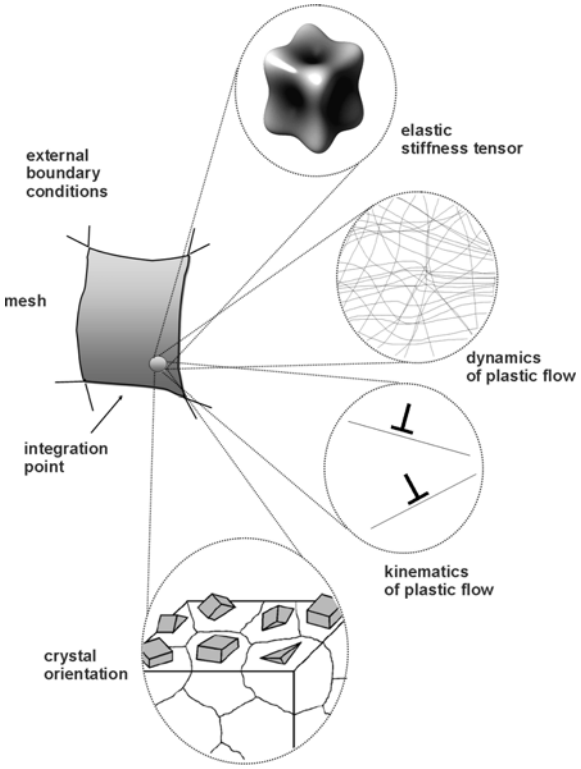

Figure 1 Principle of crystal-based finite element simulations. These methods comprise a group of continuum-based approaches which implement the tensorial nature of elastic–plastic crystalline deformation and the orientation distribution of a (poly-)crystalline aggregate.

Both topics represent important problems for the development of physically-based multi-scale models that can be used to predict thermomechanical processes and process-dependent homogenized properties of polycrystalline metals.

We use β-Ti polycrystals in this study as an example since both the crystallographic texture evolution and the texture-dependent elastic stiffness play an essential role for these materials with respect to biomedical applications.

This work is only about the role of the tensorial elastic properties in the context outlined above; the thermodynamic results obtained by DFT on the Ti–Nb binary system were published before [6].

2 Simulation procedures We studied the three binary Ti–Nb alloys Ti–18.5 at% Nb, Ti–25 at% Nb, and Ti–31.5 at% Nb. The simulation procedure was divided into two parts. First, the elastic tensor constants were calculated for the three alloys using DFT. Second, the crystallographic texture evolution under elastic–plastic plane strain loading (idealization for cold rolling) and the homogenized elastic stiffness of textured polycrystals were predicted using CPFEM and CEFEM, respectively.

2.1 Ab initio calculation using density functional theory The simulations were done using a plane wave pseudopotential approach as implemented in the Vienna Ab-initio Simulation Package (VASP) code [7–9]. The plane wave cutoff energy was 170 eV and a $8 \times 8 \times 8$ Monkhorst–Pack mesh was used to sample the Brillouin zone. In order to predict the elastic properties of the alloys, both tetragonal and trigonal deformation modes were applied to the cubic supercell. Based on the energy conservation principle, the elastic constants of the cubic systems are thus obtained. Details on the calculation of the elastic constants are presented in [10].

2.2 Crystal-based finite element method Elastic–plastic plane strain compression deformation (idealized rolling) and elastic bending of textured polycrystals were studied using CPFEM and CEFEM simulations, respectively [11–14].

The study of plane strain loading aims at the prediction of the crystallographic texture evolution as a function of the magnitude and anisotropy of the elastic stiffness tensor.

The influence of the different elastic constants on the evolution of the crystallographic deformation texture is of interest because changes in the magnitude and anisotropy of elastic stress contributions may alter the resolved shear stresses on the slip systems. This may entail different active slip system combinations and hence, different re-orientation rates of the crystals leading to changes in the deformation-induced texture evolution. The active slip systems accommodate a certain shape change of a volume element which is described via the symmetric crystallographic portion of the displacement gradient tensor. The anti-symmetric part of this tensor corresponds to the lattice re-orientation which is responsible for texture evolution. This part of the current study thus aims to investigate how sensitively texture changes depend on the elastic contribution to the local stresses.

The different elastic tensors (corresponding to the different alloys) that we use as input for the CPFEM simulations were taken from the first principles predictions outlined above. The input parameters characterizing the plastic response for the three alloys were taken from an uniaxial compression test conducted on a solution annealed Ti–30 at% Nb sample. As slip systems we used {110}, {112}, and {123} slip planes in conjunction with ⟨111⟩/2 Burgers vectors with the same critical resolved shear stress.

The CPFEM model consists of 480 elements (three-dimensional quadrilateral, eight integration points). The starting texture used for the plane strain deformation simulation is chosen to be random according to experimental observations conducted on cast samples [6, 15]. Each integration point of the FEM grid carries 4 orientations representing 4 grain portions which altogether fulfill the full-constraint Taylor homogenization condition locally at that integration point. This means that the strain constraints are homogeneous matching strain compatibility with the neighbor elements. A more detailed description of the constitutive model is given in [16, 17].

© 2008 WILEY-VCH Verlag GmbH & Co. KGaA, Weinheim

The resulting final texture (90% thickness reduction) obtained from the plane strain deformation simulation as well as the initial random texture are then both used as input orientation distributions for an elastic bending simulation. The reason for this investigation is to study the influence of crystallographic texture (plane strain deformation texture in the current case) on the overall elastic polycrystal stiffness. While the polycrystal stiffness of randomly textured material can be predicted using analytical or semi-analytical models, the corresponding overall elasticity for textured material cannot be described by analytical models but requires the use of crystal-based finite element methods.

The purpose of the elastic bending simulations is to compare the homogenized elastic properties of textured with those of non-textured (random orientation distribution) polycrystals in the case that different elastic tensors are used (in terms of magnitude and anisotropy).

The use of a crystal-based finite element method in the present context does not only provide a homogenization model for obtaining polycrystal averages of elastic data in the case of a non-random crystallographic orientation distribution but it also allows one to study details of grain-to-grain heterogeneity in metals [13]. This point is of high relevance since polycrystals do as a rule not deform homogeneously but tend to reveal strain localization and substantial inter- and intra-grain stress–strain inhomogeneity that cannot be captured by analytical approximations. Likewise is the use of ab initio predicted elastic tensor data in a CPFEM environment of high benefit since for many complex metallic alloys corresponding single crystal elastic tensor data are not available from experiments. For some metallic materials, particularly when they have a high melting point, complex chemical composition, or reveal phase transformations during cooling from the melt, single crystals cannot be produced. In such cases ab initio simulations are the only way for obtaining the elastic tensor data as input into corresponding finite element simulations.

3 Simulation results and discussion

3.1 The elastic constants calculated by DFT The elastic stiffness constants of the three Ti–Nb binary alloys obtained from DFT are shown in Table 1. The Zener ratio ($A_z = 2C_{44}/(C_{11}-C_{12})$) given in the table is a measure of the elastic anisotropy. When $A_z = 1$ the material is elastically isotropic. When A_z is larger than 1, the Young's modulus in the [111] crystallographic direction is larger than that along the [100] directions, and vice versa when $A < 1$.

Table 1 Tensor components of the elastic stiffness as predicted by DFT for three Ti–Nb alloys. E_H is the polycrystalline Young's modulus as homogenized using Hershey's homogenization model for randomly textured polycrystals [18].

composition	C_{11} (GPa)	C_{12} (GPa)	C_{44} (GPa)	A_z	E_H (GPa)
Ti–18.75 at% Nb	131.2	114.5	26.8	3.210	49.4
Ti–25 at% Nb	143.6	125.9	21.4	2.418	44.2
Ti–31.25 at% Nb	154.8	118.5	19.2	1.058	54.9

The elastic anisotropy can be visualized by the Young's modulus surface diagram, Fig. 2. In this presentation the vector direction represents the crystallographic lattice direction and its magnitude the Young's modulus. Figure 2 shows that the elastic properties become nearly isotropic with increasing Nb content.

It was pointed out by Abdel–Hady et al. [5] that when the β-phase becomes more and more stable in the Ti–Nb system, the elastic properties of the β-Ti alloy will turn gradually into those that are typical for the β-phase stabilizing alloying element itself, i.e. Nb in the present case.

Elastic modulus measurements on polycrystalline Ti–Nb binary alloys confirm that when the β-phase becomes stable, the elastic modulus of the alloy will continuously increase [19–21]. In the current DFT study, we observed the same effect, i.e. the anisotropy of elasticity becomes gradually similar to that of pure Nb which has a Zener ratio below 1 [22].

3.2 Results of the crystal plasticity finite element simulations

3.2.1 Simulation results for plane strain deformation Figure 3 shows the predicted crystallographic textures which are typical of rolled bcc metals [23]. The texture of bcc metals is typically quantified in terms of two main high symmetric orientation fibers, namely, the α-fiber which comprises all orientations with a common

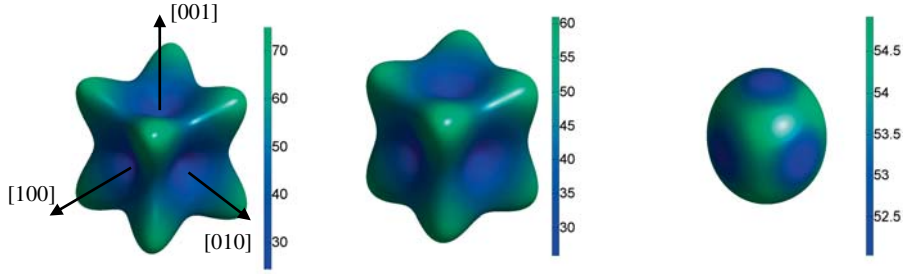

(a) (b) (c)

Figure 2 (online colour at: www.pss-b.com) Young's modulus surface plots of (a) Ti–18.75 at% Nb, (b) Ti–25 at% Nb, and (c) Ti–31.25 at% Nb.

© 2008 WILEY-VCH Verlag GmbH & Co. KGaA, Weinheim

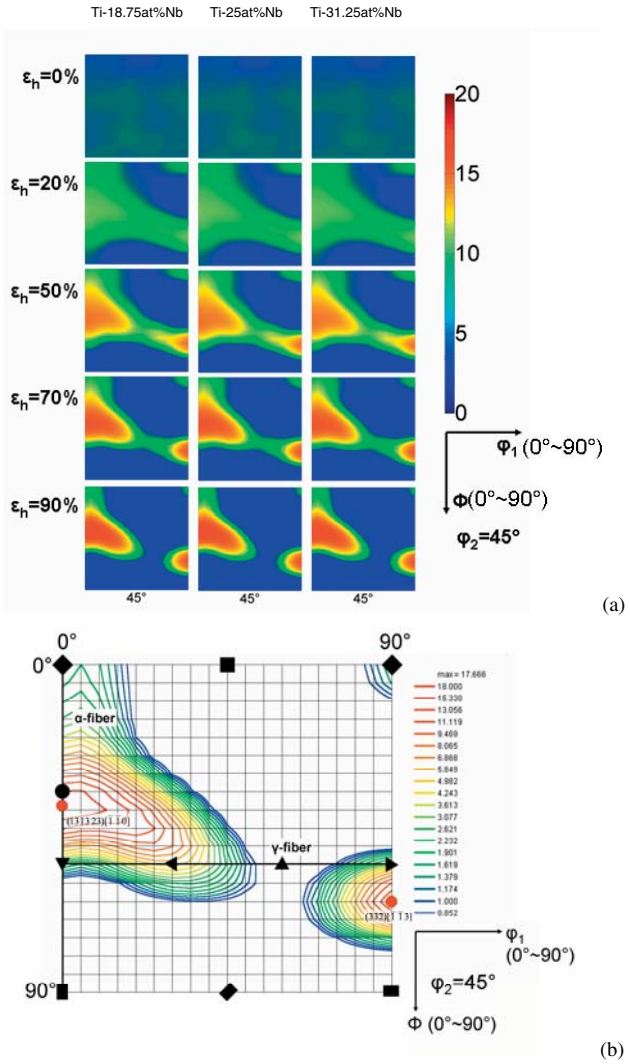

Figure 3 (online colour at: www.pss-b.com) (a) $\varphi_2 = 45°$ sections through the predicted ODFs (orientation distribution functions) of the Ti–Nb binary alloys after plane strain deformation. Left column: Ti–18.75 at%, middle column: Ti–25 at% Nb, right column: Ti–31.25 at% Nb. ε_h: engineering thickness reduction. The color code indicates the orientation density. (b) Positions of α- and γ-fibers on the ODF section of $\varphi_2 = 45°$.

crystallographic ⟨110⟩-axis parallel to the elongation direction of the plane strain tensor (rolling direction), and the γ-fiber which comprises all orientations with a common crystallographic ⟨111⟩-axis parallel to the compression direction of the plane strain tensor (sheet normal direction).

Figure 3 presents the predicted crystallographic textures in terms of a set of $\varphi_2 = 45°$ sections through Euler space for the three cases with different elastic properties. This type of orientation presentation is convenient since it contains all relevant texture information (including the α-fiber and the γ-fiber) in one single section through Euler space.

The deformation textures predicted for the three cases reveal two common features, namely, the formation of a strong, incomplete α-fibre between {001} ⟨110⟩ and {111} ⟨110⟩ and the gradual increase of the γ-fibre. For low strains {001} ⟨110⟩ and {112} ⟨110⟩ are dominant texture components on the α-fibre and a weak preference close to the {111} ⟨112⟩ becomes visible on the γ-fibre. For larger strains the maximum on the α-fibre is shifted towards ≈ {111} ⟨110⟩ and that on the γ-fibre towards {111} ⟨112⟩.

At first view the similarity among the three simulated deformation textures seems to indicate that there is principally no pronounced relationship between slip system selection and the magnitude and anisotropy of the elastic constants. This conclusion, however, is not quite admissible and deserves some reflection on the kinematic and dynamic ingredients used in such models.

Let us first consider the kinematics of the CPFEM formulation. The CPFEM boundary conditions we used in this work impose very strict strain constraints in terms of an ideal plane strain deformation state. Although in an CPFEM simulation these boundary conditions do not necessarily apply to each element but have to be fulfilled over the entire domain allowing for local strain deviations among the elements, the requirement for compatibility of the deformation field is a rather strong boundary condition. In classical plasticity homogenization theory this amounts to a Taylor–Bishop–Hill assumption. It works by prescribing for each grain an identical strain tensor, namely, that imposed externally by the tool. This boundary condition enforces identical deformation of all grains in a compatible way. This homogenization condition violates stress equilibrium among the grains since differently oriented crystals require different stress states to activate slip combinations that fulfill the same strain.

In view of the present results, where such a situation of strain dominance is approximated (of course in the current CPFEM simulation the stress equilibrium is not violated over the entire domain) one must, however, not generalize this result for the following reason: In a thought experiment we may consider a classical single crystal compression test as an example. In this case no requirement for strain compatibility among the neighbor grains exists (because there are none). The only (weak) strain constraint is the necessity that the contact between the compression tool and the sample must be preserved. Plastic flow in any other direction, however, is admissible owing to the free surface of the single crystal in any direction other than the compression direction. In such a case the necessity of stress equilibrium is more relevant than strain compatibility. It may hence be expected that for this scenario changes in the elastic properties may indeed play a role for the evolution of texture. Another point that deserves consideration in this context is the fact that the influence of changes in the elastic stresses is highly orientation dependent. This means that for some orientations (relative to an external load) small changes in the stress state may alter the active corner of the crystalline yield locus while other orientation are very stable and only large stress changes push the system into an-

© 2008 WILEY-VCH Verlag GmbH & Co. KGaA, Weinheim

other corner of the yield locus. This thought experiment (dominated by stress equilibrium, neglecting strain compatibility) is in plasticity homogenization theory referred to as Sachs hypothesis.

In other words the boundary conditions used in this study suggest that strain compatibility among the grains, as enforced by the plane strain loading and the local Taylor assumption in each element imposes a stronger boundary condition than the possibility for stress relaxation effects.

Beyond the subtleties associated with boundary conditions in homogenization theory and CPFEM simulations also dynamical aspects associated with changes in the elastic properties may play a role for texture evolution:

Modifying the elastic properties in terms of the magnitude and anisotropy changes a number of important dynamical properties associated with dislocations: First, the dislocation cores change their structure and properties. This is of high relevance for dislocation mobility and reactions. Also, changes in the dislocation core structure may have substantial influence on the applicability of Schmid's law. In BCC metals slip activity can reveal substantial twinning and anti-twinning asymmetry owing to the non-planar structure of the cores of the screw dislocations. Modifying the elastic constants can affect this structure leading to a notable change in the asymmetry of forward and backward slip [26, 27]. Second, dislocation patterning behavior will be altered. This affects the mean free path of mobile dislocations and the overall stress fields formed by ordered dislocation arrays. Both aspects are part of the CPFEM kinematics. Instead they must be considered in the constitutive models that describe strain hardening (structure evolution equations) and the relationship between microstructure and flow stress (kinetic equation of state). Since all three simulations presented in Fig. 2 used different elastic constants but the same constitutive flow stress model the only admissible conclusion from our current texture results is the following: For CPFEM simulations conducted under strain-dominated boundary conditions the kinematics associated with polycrystal texture evolution are practically independent on the elastic properties.

Beyond these mechanical considerations thermodynamic aspects can also be of relevance. Changes in the ground state of the material may alter the system in such a way that other deformation mechanisms might become relevant in β-Ti alloys such as twinning, martensite formation, or the activation of higher order slip systems, depending on the stability of the β-phase [24, 25].

3.2.2 Simulation results of the bending tests

The bending simulation was conducted as an example for calculating the effect of changes in the elastic properties on the overall elastic stiffness of textured BCC Ti–Nb polycrystals. We used the elastic tensors obtained by DFT and the textures predicted by the plane-strain loading boundary condition outlined above.

For predicting such cases the crystal elasticity finite element method is a suited approach since classical homogenization theory does not consider crystallographic textures. In this crystal-based finite element approach the overall elastic response is calculated based on the elastic tensor rotated into each respective coordinate system of all orientations under consideration of stress equilibrium and strain compatibility using a weak form approximation.

Figure 4 shows the load-displacement curves for bending of textured and non-textured binary Ti–Nb alloys. The displacement is along the negative direction of the normal direction associated with the plane strain coordinate system used above. Among the non-textured materials, Ti–25 at% Nb shows the lowest elastic modulus which is consistent with the prediction by Hershey's model (for randomly textured material) listed in Table 1. The homogenized elastic properties of textured and non-textured Ti–31.25 at% Nb are identical. This result is plausible since the Zener ratio of this material is almost 1 which

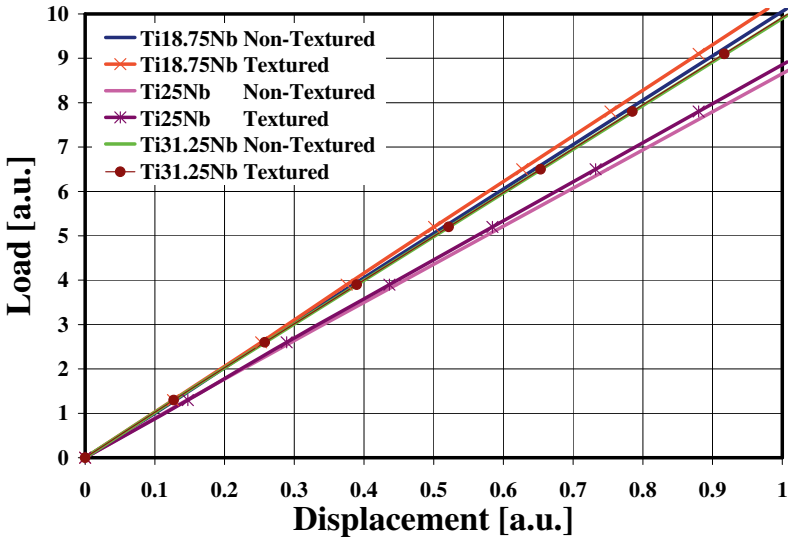

Figure 4 (online colour at: www.pss-b.com) Simulated load-displacement curves obtained for the elastic bending tests for textured and non-textured BCC Ti–Nb polycrystals. The predictions were made using the crystal elasticity finite element method. Compositions are given in at%.

© 2008 WILEY-VCH Verlag GmbH & Co. KGaA, Weinheim

means that the elastic properties are practically isotropic. Consequently, no difference exists between the overall polycrystal stiffness of textured and non-textured material.

The largest change in the elastic polycrystal properties between textured and non-textured material occurs for Ti-18.75 at% Nb. This material has the largest Zener ratio of the three alloys. The difference of the overall elastic moduli between the textured and non-textured material is close to 5%.

3.2.3 Combination of DFT and CPFEM In this study we have integrated elastic modulus data from an ab initio modeling (DFT) in continuum-based crystal mechanical finite element simulations (CPFEM) to predict crystallographic textures and texture-dependent polycrystal elastic stiffness. The approach is applied to the elastic properties of β-phase Ti–Nb binary alloys which represent an important biomaterial class for human implant design.

The two models we combine (DFT, CPFEM) work at very different length and time scales. The strength of this combination for predicting certain polycrystal properties lies in the fact that continuum-based theoretical models such as CPFEM rely on a number of ground state properties (e.g. elastic tensor) the value of which does not depend on the microstructural path of the material. The use of texture data is sufficient to predict realistic data also for complex polycrystalline aggregates irrespective of their thermo-mechanical process history. This is particularly evident for the elastic bending problem we discussed above.

A particular advantage of using an FEM based methods rather than an analytical or semi-analytical approach for obtaining the polycrystal stiffness from corresponding DFT single crystal data is that it allows one to consider any kind of crystallographic texture including also intra- or in-grain interactions. Most homogenization methods for obtaining the elastic modulus of a polycrystal such as the Voigt, Reuss, Hill, or Hershey models usually either neglect texture or assume highly simplified boundary conditions. This is not necessary in the case of a crystal-based FEM method where each integration point or element can assume an individual crystallographic orientation [16, 17, 28].

The combination of the two methods (DFT, CPFEM) provided very promising results also for the elastic-plastic deformation problem of deformation-induced texture evolution. It must be realized, however, that plasticity is a highly dynamic and path-dependent problem which requires further atomic-based input than just the elastic constants. As discussed above the change in the elastic properties goes along with corresponding changes in the microscopic dislocation behavior.

A further very important aspect of using DFT in conjunction with crystal mechanical simulations is the fact that for the elastic constants of single crystals (which are a necessary input to CPFEM simulations) experimental data is often lacking owing to the reasons outlined in Section 2.2.

Table 2 Suitable interfaces between DFT and CPFEM/CEFEM.

DFT	CPFEM/CEFEM	aim
phases and composition in thermodynamic equilibrium	homogenized mechanical response of textured multi-grain and multi-phase aggregates; Intra- and inter-phase mechanics, mechanics at internal interfaces	single or multi-phase mechanics; texture evolution
elastic constants	elastic constants of textured polycrystals	elastic stiffness and anisotropy
stacking fault energy, critical resolved shear stress	flow law for textured multi-grain and multi-phase aggregates	materials strength

In summary we can state that we presented a concept of combining DFT and CPFEM simulations. DFT and CPFEM are both well established approaches but they are up to now used for different purposes in different scientific communities. While DFT methods are used at the electronic scale, CPFEM and CEFEM methods are applied to tackle problems of crystal-scale mechanics. As we demonstrated DFT methods can predict thermodynamic ground state properties such as elastic tensors of perfect single crystals. For predicting polycrystal properties the behavior of the single crystals must be averaged which can be done by CPFEM models also in the case of non-random orientation distributions. Since CPFEM and CEFEM are continuum-scale approximations, they require data for the parameters of the underlying constitutive laws. These can be obtained from DFT calculations. Possible areas of interfacing these two approaches are summarized in Table 2.

4 Conclusions The elastic tensors of three β-phase (BCC) Ti–Nb binary alloys (Ti–18.5 at% Nb, Ti–25 at% Nb, and Ti–31.5 at% Nb) were predicted by ab initio (DFT) calculations and used as input for crystal plasticity and crystal elasticity finite element simulations (CPFEM). The main results are:

1. The ab initio calculations of the single-crystal cubic elastic constants revealed a strong compositional dependence of the magnitude and elastic anisotropy. Ti–18.5 at% Nb reveals the strongest elastic anisotropy. Ti–31.5 at% Nb is nearly isotropic.

2. The elastic properties for the three alloys were used as input to CPFEM-based elastic-plastic deformation texture simulations using ideal plane strain boundary conditions (idealized cold rolling). The resulting orientation distributions were practically identical. This result was interpreted in terms of the strong dominance of strain compatibility for texture formation under such kinematical constraints. It was discussed that generalization to single crystal plasticity under stress dominated boundary conditions is not recommendable.

3. The elastic single crystal tensors obtained by DFT were used for calculating the overall stiffness for the three polycrystalline alloys (textured and non-textured) for elas-

© 2008 WILEY-VCH Verlag GmbH & Co. KGaA, Weinheim

tic bending conditions. The strong single crystal anisotropy of Ti–18.5 at% Nb was less pronounced in case of the polycrystalline material due to mutual elastic compensation effects. The occurrence of texture (obtained from the plane strain simulation) leads to about 5% difference in stiffness when compared to the randomly oriented material. For the isotropic material no texture dependence of the elastic polycrystal stiffness occurs.

4. We could demonstrate a scale-bridging simulation concept that combines ab initio modeling with crystal-based finite element homogenization. The method was applied to two examples, namely to the prediction of texture evolution (DFT in conjunction with the crystal plasticity finite element method) and elastic bending of textured and non-textured polycrystals (DFT in conjunction with the crystal elasticity finite element method).

References

[1] P. Hohenberg and W. Kohn, Phys. Rev. **136**, B864 (1964).
[2] W. Kohn and L. J. Sham, Phys. Rev. **140**, A1133 (1965).
[3] M. Long and H. J. Rack, Biomaterials **19**, 1621 (1998).
[4] M. Morinaga, N. Yukawa, T. Maya, K. Sone, and H. Adachi, 6th World Conference on Titanium, France (1988).
[5] M. Abdel-Hady, K. Hinoshita, and M. Morinaga, Scr. Mater. **55**, 477 (2006).
[6] D. Raabe, B. Sander, M. Friák, D. Ma, and J. Neugebauer, Acta Mater. **55**, 4475 (2007).
[7] G. Kresse and J. Hafner, Phys. Rev. B **47**, 558 (1993).
[8] G. Kresse and J. Furthmüller, Phys. Rev. B **54**, 11169 (1996).
[9] P. E. Blöchl, Phys. Rev. B **50**, 17953 (1994).
[10] K. Chen, L. R. Zhao, and J. S. Tse, J. Appl. Phys. **93**, 2414 (2003).
[11] D. Raabe, Z. Zhao, and F. Roters, Scr. Mater. **50**, 1085 (2004).
[12] D. Raabe, Z. Zhao, and W. Mao, Acta Mater. **50**, 4379 (2002).
[13] D. Raabe, M. Sachtleber, Z. Zhao, and D. Raabe, Mater. Sci. Eng. A **336**, 81 (2002).
[14] D. Raabe, P. Klose, B. Engl, K.-P. Imlau, F. Friedel, and F. Roters, Adv. Eng. Mater. **4**, 169 (2002).
[15] B. Sander and D. Raabe, Mater. Sci. Eng. A **479**, 236 (2008).
[16] D. Raabe and F. Roters, Intern. J. Plast. **20**, 339 (2004).
[17] Z. Zhao, F. Roters, W. Mao, and D. Raabe, Adv. Eng. Mater. **3**, 984 (2001).
[18] A. V. Hershey, J. Appl. Mech. **21**, 236 (1954).
[19] S. G. Fedotov and P. K. Belousov, Phys. Met. Metallogr. **17**, 83 (1964).
[20] M. Lee, C. P. Ju, and J. H. Chern Lin, J. Oral Rehabil. **29**, 314 (2002).
[21] H. Matsumoto, S. Watanabe, N. Masahashi, and S. Hanada, Metall. Mater. Trans. A **37**, 3239 (2006).
[22] W. F. Hosford, The Mechanics of Crystals and Textured Polycrystals (Oxford University Press, New York/Oxford, 1993).
[23] M. Hölscher, D. Raabe, and K. Lücke, Steel Res. **62**, 567 (1991).
[24] W. Xu, K. B. Kim, J. Das, M. Calin, and J. Eckert, Scr. Mater. **54**, 1943 (2006).
[25] S. Hanada, M. Ozeki, and O. Izumi, Metall. Mater. Trans. A **16**, 789 (1985).
[26] A. Seeger and W. Wasserbäch, phys. stat. sol. (a) **189**, 27 (2002).
[27] V. Vitek, Cryst. Lattice Defects **5**, 1 (1974).
[28] P. Eisenlohr and F. Roters, Comput. Mater. Sci. **42**, 670 (2008).

© 2008 WILEY-VCH Verlag GmbH & Co. KGaA, Weinheim